

THE DATA TRANSFER KIT: A GEOMETRIC RENDEZVOUS-BASED TOOL FOR MULTIPHYSICS DATA TRANSFER

S.R. Slattery and P.P.H. Wilson

Department of Engineering Physics
University of Wisconsin - Madison
1500 Engineering Dr., Madison, WI 53706
sslattery@wisc.edu; wilsonp@engr.wisc.edu

R.P. Pawlowski

Sandia National Laboratories*
P.O. Box 5800, Albuquerque, NM 87185
rppawlo@sandia.gov

ABSTRACT

The Data Transfer Kit (DTK) is a software library designed to provide parallel data transfer services for arbitrary physics components based on the concept of geometric rendezvous. The rendezvous algorithm provides a means to geometrically correlate two geometric domains that may be arbitrarily decomposed in a parallel simulation. By repartitioning both domains such that they have the same geometric domain on each parallel process, efficient and load balanced search operations and data transfer can be performed at a desirable algorithmic time complexity with low communication overhead relative to other types of mapping algorithms. With the increased development efforts in multiphysics simulation and other multiple mesh and geometry problems, generating parallel topology maps for transferring fields and other data between geometric domains is a common operation. The algorithms used to generate parallel topology maps based on the concept of geometric rendezvous as implemented in DTK are described with an example using a conjugate heat transfer calculation and thermal coupling with a neutronics code. In addition, we provide the results of initial scaling studies performed on the Jaguar Cray XK6 system at Oak Ridge National Laboratory for a worse-case-scenario problem in terms of algorithmic complexity that shows good scaling on $O(1 \times 10^4)$ cores for topology map generation and excellent scaling on $O(1 \times 10^5)$ cores for the data transfer operation with meshes of $O(1 \times 10^9)$ elements.

Key Words: data transfer, multiphysics, rendezvous algorithm, parallel computing

1. INTRODUCTION

In many physics applications, it is often desired to transfer fields (i.e. degrees of freedom or other data) between geometric domains that may or may not conform in physical space. In addition, for massively parallel simulations, it is typical that geometric domains not only do not conform spatially, but also that their parallel decompositions do not correlate and are independent of one another due to physics-based partitioning and discretization requirements. As an example, this situation can occur in multiphysics simulations where physics fields provide feedback between solution iterations [1] or parallel adaptive mesh simulations where fields must be moved between meshes after refining and coarsening [2]. It is therefore

*Sandia National Laboratories is a multi-program laboratory managed and operated by Sandia Corporation, a wholly owned subsidiary of Lockheed Martin Corporation, for the U.S. Department of Energy's National Nuclear Security Administration under contract DE-AC04-94AL85000.

desirable to have a set of tools to relate two geometric domains of arbitrary parallel decomposition such that fields and other data can be transferred between them.

The Data Transfer Kit (DTK) is a software library developed as part of the Consortium for Advanced Simulation of LWR's (CASL) [3] designed to provide parallel services for mesh and geometry searching and data transfer. The algorithms implemented in DTK are based on the concept of geometric rendezvous as developed by Plimpton, Hendrickson, and Stewart [4] originally implemented as part of the SIERRA framework [5]. Their work has been extended to move towards a component design for use with arbitrary physics codes such that varying representations of mesh, geometry, and fields are able to access these services [6]. In addition, the original mesh-based rendezvous algorithms have been expanded to be used with both mesh and geometry representations of the geometric domain. This document will briefly outline the rendezvous algorithms as implemented in DTK. An example of data transfer using a conjugate heat transfer calculation and a thermal-neutronics type coupling is provided. Parallel scaling results are also presented for the mesh-based mapping algorithm for a worse-case-scenario problem where communication costs are at a maximum.

2. GEOMETRIC RENDEZVOUS

Relating two non-conformal meshes will ultimately require some type of data evaluation algorithm to apply the data from one geometry to another. To drive these evaluation algorithms, the target objects to which this data will be applied must be located within the the source geometry. In a serial formulation, efficient search structures that offer logarithmic asymptotic time complexity are available to perform this operation. However, in a parallel formulation, if these two geometries are arbitrarily decomposed, geometric alignment is not likely and a certain degree of parallel communication will be required. A geometric rendezvous manipulates the source and target geometries such that all geometric operations and data evaluation operations have a local formulation while data transfer occurs globally.

A geometry that is providing data through evaluations will be referred to as the source geometry while the geometry that will be receiving the data will be referred to as the target geometry. Although explicitly formulated with a source mesh and target vertices below, these concepts can be applied to geometric structures beyond mesh and vertices.

2.1. Rendezvous Decomposition

The geometric rendezvous concept uses a global formulation for the data transfer while maintaining a local formulation for the geometric search operations by generating a secondary decomposition of the geometric structures in the problem. This secondary decomposition is generated by a geometry-based repartitioning for more load-balanced searching algorithms. This repartitioning is shown in the example presented in Figure 1 where two meshes, one of triangles and one of quadrilaterals, are decomposed into four partitions, shown by color, that are not correlated to one another. To transfer data between these meshes, each partition in both meshes will need to communicate data to each partition in the other mesh due to their geometric overlap. The rendezvous decomposition, shown on the right, is a geometrically balanced repartitioning of the source mesh in the transfer problem with the partitioning information shared amongst both meshes. The components of both meshes that are required for data transfer will be gathered into this new partition.

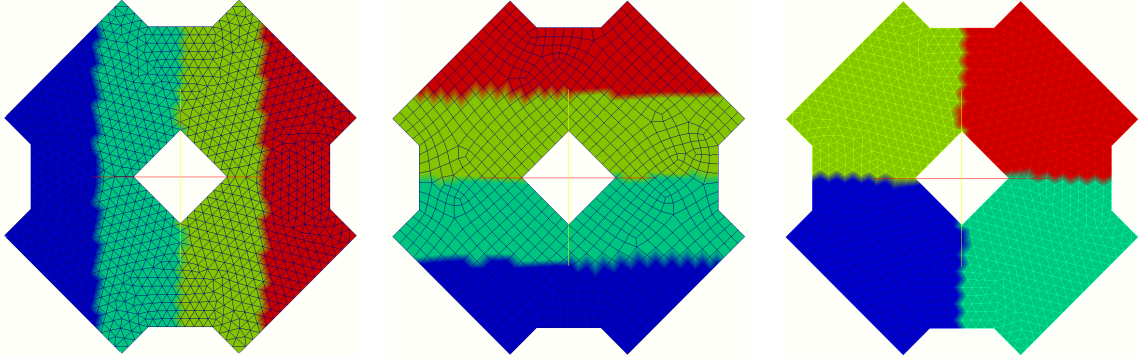


Figure 1. Rendezvous decomposition example. A triangle mesh (left) and a quadrilateral mesh (center) are partitioned into 4 parallel domains as indicated by color. The rendezvous decomposition (right) is generated as a geometric-based repartitioning of the source mesh that permits load balanced geometric operations.

In DTK, the rendezvous algorithm developed by Plimpton et. al. [4] for mesh-based data transfer generates the rendezvous decomposition which behaves as a hierarchical parallel and geometric search tree. Using this algorithm, a secondary decomposition of a subset of the source mesh that will participate in data transfer is generated, forming the rendezvous decomposition as described in the example above. The rendezvous decomposition is encapsulated as a separate entity from the original geometric description of the domain. It can be viewed as a temporary copy of the source mesh subset that intersects the target geometry.

With the rendezvous decomposition, we effectively have a search structure that spans both parallel and physical space. We first search parallel space by querying the rendezvous decomposition generated during repartitioning. Global recursive coordinate bisectioning parameters are maintained for global partitioning information, meaning that a destination process in the rendezvous decomposition can be determined for any point on any process [7]. Although this is a search over parallel space, because of the geometric nature of the rendezvous decomposition it is also a search over physical space with each process in the rendezvous decomposition owning a specific subset of the mesh (with marginal overlap at the boundaries).

Once points have been accumulated in the rendezvous decomposition, the local kD-tree that is formed over the local mesh can be utilized. By searching the kD-tree in logarithmic time, a subset of the mesh that is in the vicinity of the target point is generated [8]. This subset, which is typically much smaller than the mesh owned by a particular rendezvous process, is then searched with a more expensive point-in-element operation that transforms the point into the reference frame of each mesh element in the subset with a Newton iteration strategy. This mapped point is then checked against the canonical reference cell of that mesh element's topology to determine if the point is contained within.

2.2. Parallel Topology Maps

A set of mapping algorithms based on geometric rendezvous are implemented within DTK that apply specifically to shared domain problems. A shared domain problem is one in which the geometric domains of the source and target intersect over all dimensions of the problem. Figure 2 gives an example of a shared domain problem in 3 dimensions. Here, $\Omega(S)$ (yellow) is the source geometry, $\Omega(T)$ (blue) is the target geometry, and $\Omega(R)$ (red) is their intersection and the shared domain over which mapping and the rendezvous decomposition will be generated. The purpose of these mapping algorithms is to efficiently

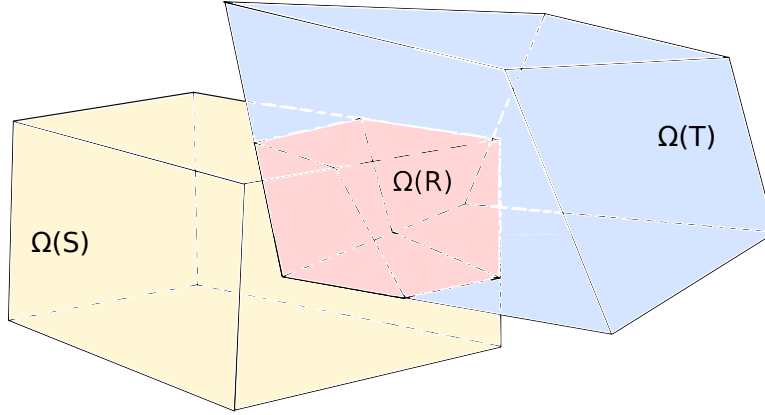


Figure 2. Shared domain example. $\Omega(S)$ (yellow) is the source geometry, $\Omega(T)$ (blue) is the target geometry, and $\Omega(R)$ (red) is the shared domain.

generate a parallel topology map and the associated parallel communication plan that can carry out the data transfer repeatedly with the minimum required number of parallel messages and data. A parallel topology map is an operator, M , that defines the translation of a field, $F(s) : \mathbb{R}^D \rightarrow \mathbb{R}^N$, from a source spatial and parallel domain, Ω_S , to a field, $G(t) : \mathbb{R}^D \rightarrow \mathbb{R}^N$, in the target spatial and parallel domain Ω_T , such that $G(t) \leftarrow M(F(s))$ and $M : \mathbb{R}^N \rightarrow \mathbb{R}^N, \forall r \in [\Omega_S \cap \Omega_T]$, where N is the dimensionality of the field and D the dimensionality of the spatial domain. It then follows that the geometric rendezvous is defined as a geometric-based parallel redistribution of the original source and target geometries defined over the region $\Omega_R = \Omega_S \cap \Omega_T$.

These maps are generated by creating source/target pairs found by searching the rendezvous decomposition. For each target object for which data are desired, the rendezvous decomposition is searched with that object to find the corresponding source object. In the case of finite element interpolation, the target object would be a quadrature point in the target finite element mesh and the source object would be a source element in the source finite element mesh that contains the target point. The map would then drive the field evaluation, $G(t) \leftarrow M(F(s))$, for all source/target pairs. Embedded within the map is a communication plan that describes the communication sequence for transferring the data from the source geometry to the target geometry. Once the field evaluations are complete, the communication sequence moves that data from the source geometry decomposition to the target geometry decomposition to complete the data transfer and the application to the map operator.

2.3. Extension to General Geometries

To handle software components that have a geometric entity-based representation (e.g. a sub-channel code discretized with a control volume approach representing the geometry), the above algorithms have been extended to operate on a general geometric description. The mesh-based algorithm above is purely geometric, with each element in the mesh treated as a separate geometric entity. If this is the case, then other geometries such as annular rings, cubes, or any other irregular shapes should apply to the algorithm. To extend the above algorithm, we require a geometric entity to provide a small set of information including point inclusion tests, the bounding box of the entity, centroid, and dimensionality. With this information, the RCB partitioning can be generated and the geometry repartitioned to the rendezvous decomposition. With the repartitioned geometry data we can then perform a proximity search followed by

the more expensive point inclusion checks.

Given these new search structures, variations of the algorithms presented in [4] can be generated to apply to data transfer problems beyond mesh-based interpolation. DTK includes a geometric data evaluation algorithm, very similar to the original algorithm where data is applied to points in the domain based on the field discretization in the geometry rather than mesh elements. Geometry-to-geometry transfers are available when the two physics components being coupled derive their geometric description from the same source. This is useful in cases such as transferring fuel temperatures from a geometric zone in one physics application to the same geometric zone in another application. Finally, for cases where volume-averaged quantities are desired, typically an integral is evaluated over some volume of space. To support these operations, DTK contains algorithms for integrating mesh-based fields over the geometry that the mesh has discretized, providing an effective means for integral assembly mesh-to-geometry transfers.

3. DATA TRANSFER EXAMPLE USE CASE

This section demonstrates an important DTK use case for CASL. A goal of the CASL program [3] is to develop an advanced simulator capability for a pressurized light water reactor core. To achieve this, two large-scale parallel codes have been coupled using DTK, a thermal hydraulics (TH) code [9] and a neutronics (NE) code [10]. The TH code performs a multiphysics conjugate heat transfer simulation where energy conservation equation is solved in the fuel pins and energy, momentum and mass conservation equations are solved in the fluid surrounding the fuel pins. The TH simulation uses fully coupled fully implicit Newton-Krylov solvers with algebraic multigrid preconditioning [11]. The NE code uses a discrete ordinates solution to the radiation transport equation with both energy and spatial domain decomposition to achieve high levels of parallelism. In this coupling, DTK is leveraged to transfer data in parallel between the codes and a simple block Gauss-Siedel iteration loop is used to converge the global coupled system. Both physics codes have been demonstrated to run on leadership class machines with greater than 100,000 cores.

The solution is spatially distributed across processes, requiring the use of DTK to identify and execute an efficient communication plan for data transfer. For NE to TH coupling, the NE code supplies source terms used by the energy conservation equation in the fuel pins of the TH code. A point-to-point data transfer is required where the TH code requires source term values at the quadrature points for the finite element integration with the mapping generated by the DTK mesh-to-mesh rendezvous capability. For TH to NE coupling, the TH code supplies average temperatures for a section of the fuel pin to the NE code for the cross-section calculations. The DTK mesh-to-geometry integral assembly mapping is used to provide cell integrated contributions to the total average temperature for the geometric entity (fuel pin section). Sample 2D verification simulations from this work are provided in the following section.

3.1. Data Transfer Verification

A simplified form of the full physics simulation was used to verify the parallel data transfer. An analytic solution for the source term was prescribed in the NE code and transferred to the TH code. The simulation was performed on 10 cores with TH using 5 cores and NE using the remaining 5 cores. Figure 3 shows the parallel decomposition for each application code with the TH heat transfer and fluid domains shown in Figure 4 on the left. Note that the NE code uses a structured mesh while the TH code uses an unstructured mesh. Results showed that data was transferred correctly with machine precision accuracy using DTK. A plot of the transferred verification function (source = $x * y$) is shown in Figure 4 on the right.

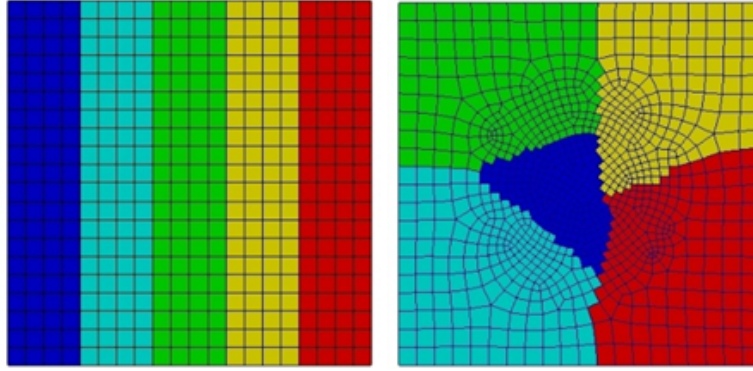


Figure 3. Parallel decomposition for coupled NE/TH verification. The colors indicate ownership of the element by a core. In this example, a 10 core job is run with the thermal hydraulics and neutronics applications each owning 5 cores on separate processor spaces.

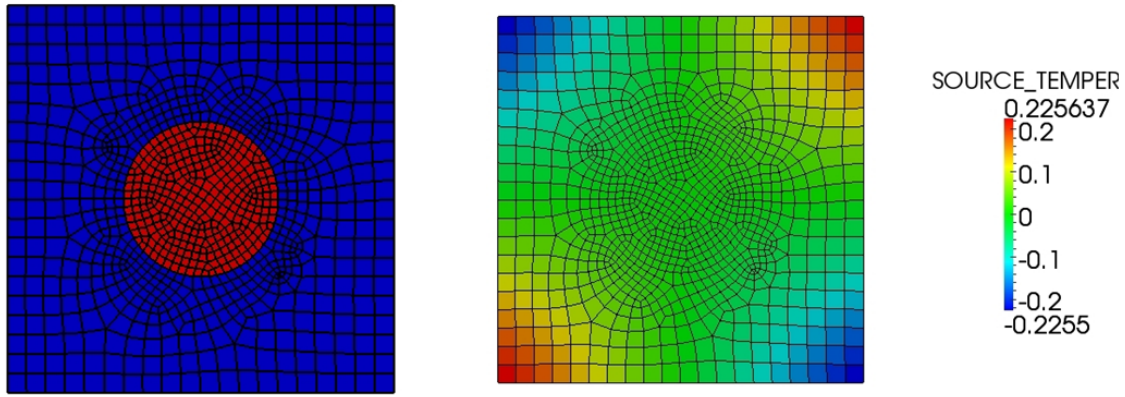


Figure 4. (Left) Verification simulation domain space consisting of a top-down view of a single fuel pin surrounded by a fluid region. The blue region represents the fluid area and the red region represents the solid fuel pin. (Right) Multiphysics domain space.

4. PARALLEL SCALING STUDY

As indicated by the CASL use cases above, the current physics codes leveraged scale to leadership class computing facilities. A typical use case of DTK in these cases is searching a mesh with a set of points and applying field data to those points through function evaluations. For this use case, a scaling study of the mesh-based DTK implementation of the rendezvous algorithm for data transfer was performed utilizing the Jaguar Cray XK6 system at Oak Ridge National Laboratory in order to assess performance at these high levels of parallelism. For each study, a tri-linear hexahedron mesh was generated to represent the source and decomposed across the parallel domain. Each partition had one element in the z direction while the x and y directions were varied to produce the desired number of elements in the partition. All source mesh partitions in each scaling study are square. To simulate a worst-case problem from an algorithmic complexity perspective, a surrogate target mesh with vertices partitioned at random is generated by sampling the x and y directions over the full global mesh domain. The result of the random parallel partitioning of target mesh vertices is that each parallel process will asymptotically contain target mesh vertices that exist in the geometrically partitioned source mesh on all processes. Each process will be guaranteed a unique set of random target mesh vertices by striding the random number seed used to

generate the vertex coordinates. For each scaling study, every process generated the same number of random vertices as the number of elements on that process, ensuring that a dense, all-to-all communication operation will be required for mapping and data transfer. Once the target vertices are mapped to the source mesh, the data transfer routine applies the process rank in which they were found and transfers it back to the original owning process for the vertex. In this way, because of the simple partitioning used for the scaling studies, the results of the data transfer to the random vertices can be independently verified by checking the applied data against the expected mesh process rank.

4.1. Weak Scaling

For the weak scaling study, the number of hexahedrons and random target vertices per partition was fixed to 1×10^4 . The number of cores used varied from 16 to 115,072. Figure 5 gives the results of the weak scaling study. The largest case reported here uses 115,072 cores and required 10.44 minutes for map generation and 0.48 seconds for data transfer with a mesh size of 1.15×10^9 elements. It is clear from the weak scaling study that at high numbers of processors communication latency begins to dominate for this dense all-to-all problem as described above. However, it is worth noting that once the mapping is complete, wall time for the actual transfer of the data is several orders of magnitude less.

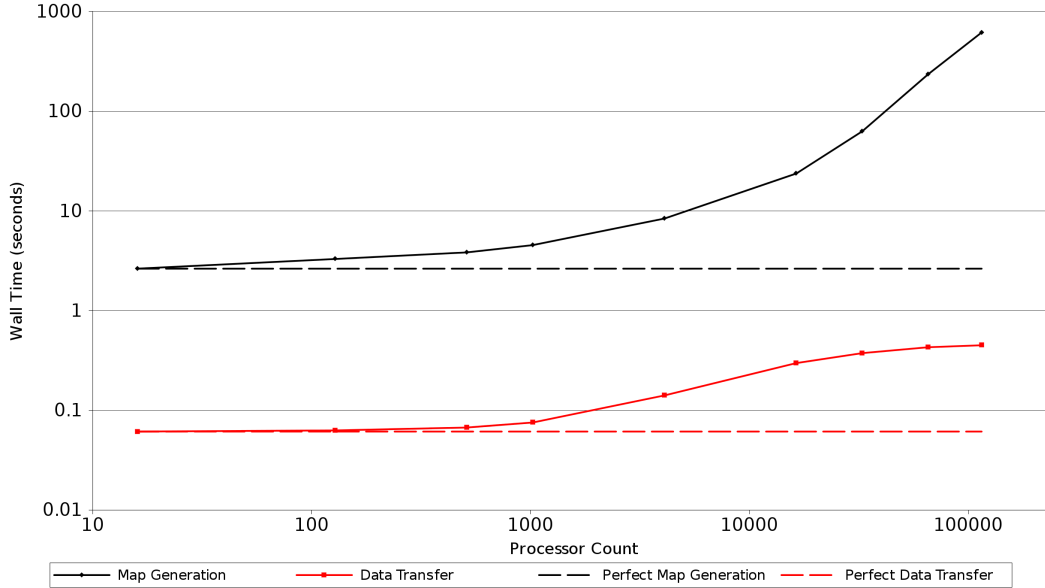


Figure 5. Weak scaling study results. The solid black curve reports the wall time to generate the mapping vs. number of processors while the solid red curve reports the wall time to transfer the data vs. number of processors. The dashed lines give perfect weak scaling the map generation (black) and the data transfer (red).

Table I gives the raw data for the weak scaling study. We note here that both the map generation time and the data transfer time are relatively load balanced with average compute times reported near the maximum compute time. In addition it should be noted that for even the largest case at 115,072 cores the wall time is not prohibitively large with the map generation routine requiring approximately 10.44 minutes and the data transfer routine requiring less than half a second.

The efficiency values for the map generation and data transfer routines are also reported in Table II with the

16 core case used as the reference computation. In correlation with the data presented in Table I, the efficiencies are observed to be low above 1,000 cores for this dense all-to-all communication problem. For more physical coupling problems where the communication is expected to be much sparser, this gives an idea of just how sparse that communication must be for this algorithm to scale well.

| Cores | Global Elements | Map Min (s) | Map Max (s) | Map Average (s) | Transfer Min (s) | Transfer Max (s) | Transfer Average (s) |
|---------|-----------------|-------------|-------------|-----------------|------------------|------------------|----------------------|
| 16 | 1.600E+05 | 2.63 | 2.65 | 2.635 | 0.06 | 0.07 | 0.062 |
| 128 | 1.280E+06 | 3.25 | 3.31 | 3.30 | 0.06 | 0.07 | 0.063 |
| 512 | 5.120E+06 | 3.58 | 3.86 | 3.84 | 0.06 | 0.08 | 0.067 |
| 1,024 | 1.024E+07 | 3.98 | 4.53 | 4.48 | 0.06 | 0.09 | 0.076 |
| 4,096 | 4.096E+07 | 6.54 | 8.51 | 8.39 | 0.13 | 0.15 | 0.141 |
| 16,384 | 1.638E+08 | 15.98 | 27.0 | 23.73 | 0.28 | 0.32 | 0.296 |
| 32,768 | 3.277E+08 | 40.03 | 68.18 | 62.88 | 0.36 | 0.39 | 0.375 |
| 65,536 | 6.554E+08 | 214.69 | 239.21 | 234.76 | 0.41 | 0.45 | 0.429 |
| 115,072 | 1.151E+09 | 570.12 | 626.51 | 616.675 | 0.42 | 0.48 | 0.450 |

Table I. Weak scaling study data with the local problem size fixed to $1.0E4$ elements/points. All times reported in seconds. Minimum, maximum, and average timing values are global and computed using the results from all processes.

| Cores | Map Efficiency | Transfer Efficiency |
|---------|----------------|---------------------|
| 16 | 1.000 | 1.000 |
| 128 | 0.800 | 0.974 |
| 512 | 0.687 | 0.911 |
| 1,024 | 0.581 | 0.812 |
| 4,096 | 0.314 | 0.434 |
| 16,384 | 0.111 | 0.206 |
| 32,768 | 0.042 | 0.164 |
| 65,536 | 0.011 | 0.143 |
| 115,072 | 0.004 | 0.136 |

Table II. Weak scaling efficiencies. The 16 process case was used as the reference case.

Compared to the weak scaling results observed by Plimpton and colleagues for a similar dense communication problem [4], these results show the same qualitative behavior (see figure 7 in the reference). As the Jaguar system improves on all aspects of machine performance over those used in the 2004 work, it is expected that larger problems may be solved before the bandwidth limiting behavior is observed.

4.2. Strong Scaling

For the strong scaling study, the global number of hexahedrons and random target vertices was fixed to 1×10^8 with the number of cores varied from 256 to 65,536. Figure 6 gives the results of the strong scaling study. Again, we note for the all-to-all communication pattern required to map the random vertices that

latency again begins to dominate when a few thousand cores are used while the data transfer scaling is excellent. The raw data for this study is presented in Table III. We see again that the algorithm is relatively load balanced with average compute times near the maximum reported compute times for the map generation operation. Table IV gives the efficiencies computed for the strong scaling study with the 256 processor case used as the reference.

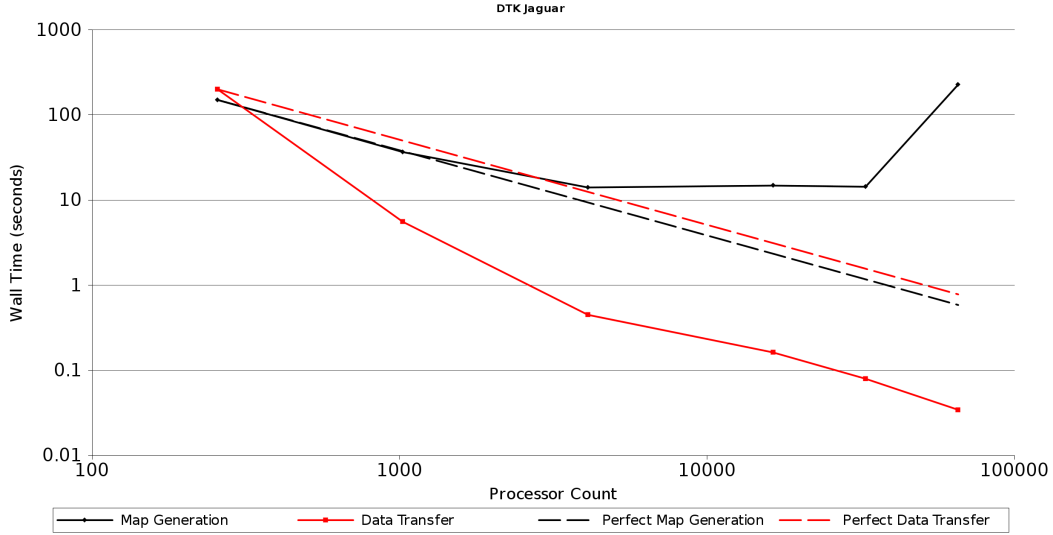


Figure 6. Strong scaling study results. The solid black curve reports the wall time to generate the mapping vs. number of processors while the solid red curve reports the wall time to transfer the data vs. number of processors. The dashed lines give perfect strong scaling the map generation (black) and the data transfer (red).

| Cores | Local Elements | Map Min (s) | Map Max (s) | Map Average (s) | Transfer Min (s) | Transfer Max (s) | Transfer Average (s) |
|--------|----------------|-------------|-------------|-----------------|------------------|------------------|----------------------|
| 256 | 3.91E+05 | 149.58 | 150.04 | 149.883 | 198.99 | 199.81 | 199.72 |
| 1,024 | 9.77E+04 | 36.08 | 36.68 | 36.60 | 5.52 | 5.59 | 5.55 |
| 4,096 | 2.44E+04 | 12.12 | 14.18 | 14.0558 | 0.37 | 0.45 | 0.04 |
| 16,384 | 6.10E+03 | 9.16 | 15.75 | 14.787 | 0.15 | 0.18 | 0.162 |
| 32,768 | 3.05E+03 | 7.42 | 17.92 | 14.33 | 0.06 | 0.10 | 0.080 |
| 65,536 | 1.53E+03 | 205.54 | 232.01 | 227.07 | 0.02 | 0.05 | 0.034 |

Table III. Strong scaling study data. All times reported in seconds. Minimum, maximum, and average timing values are global and computed using the results from all processes.

5. CONCLUSIONS

We have presented the Data Transfer Kit, a new tool for parallel data transfer for multiphysics applications. The concept of geometric rendezvous is used to provide a collection of mesh and geometry-based mappings for data transfer in shared domain problems. Initial scaling studies have been completed for the Data Transfer Kit on the Jaguar Cray XK6 system. Their results show comparable qualitative behavior to the literature results with improved performance due to the more advanced computational resources

| Cores | Map Efficiency | Transfer Efficiency |
|--------|----------------|---------------------|
| 256 | 1.000 | 1.000 |
| 1,024 | 1.024 | 8.989 |
| 4,096 | 0.666 | 27.84 |
| 16,384 | 0.158 | 19.24 |
| 32,768 | 0.082 | 19.62 |
| 65,536 | 0.003 | 22.71 |

Table IV. Strong scaling efficiencies. The 256 process case was used as the reference case.

available with good scaling for the data transfer operation at $O(1 \times 10^5)$ cores. However, for the dense communication patterns required to complete the scaling study problem, poor weak scaling results are still observed above $O(1 \times 10^4)$ cores for the mapping operation. For data transfer problems where the underlying mesh or geometry does not change, the wall times observed for the mapping algorithm to be performed may not be prohibitive as that operation will only be performed once during a setup phase for the problem. Once the map is generated, it and the resulting parallel communication plan can be used repeatedly in the data transfer operation with excellent scaling and minimal wall time observed for meshes of $O(1 \times 10^9)$ elements.

It is expected for more physical data transfer problems that the overall communication pattern will be significantly sparser than the problem presented here. Because of this, scaling for the mapping algorithm is expected to improve for more physical problems. Further scaling studies will be required to test this hypothesis. In addition, Data Transfer Kit has the potential to be extended to provide surface-to-surface mappings for interface data transfers.

ACKNOWLEDGEMENTS

This work was performed under funding provided by the Consortium for Advanced Simulation of Light Water Reactors (CASL). The authors would like to thank the CASL Virtual Reactor Integration (VRI) development team for their assistance over the course of development of DTK and the Oak Ridge Leadership Computing Facility (OLCF) for providing computational resources and support.

REFERENCES

- [1] T. Tautges and A. Caceres, “Scalable parallel solution coupling for multiphysics reactor simulation,” *Journal of Physics: Conference Series*, vol. 180, pp. 1–5, 2009.
- [2] H. Edwards, “Managing complexity in massively parallel, adaptive, multiphysics applications,” *Engineering with Computers*, vol. 22, pp. 135–155, 2006.
- [3] U.S. Department of Energy, “CASL - a project summary,” CASL-U-2011-0025-000, Consortium for Advanced Simulation of LWRs, 2011.
- [4] S. Plimpton, B. Hendrickson, and J. Stewart, “A parallel rendezvous algorithm for interpolation between multiple grids,” *Journal of Parallel and Distributed Computing*, vol. 64, pp. 266–276, 2004.

- [5] J. Stewart and H. Edwards, “A framework approach for developing parallel adaptive multiphysics applications,” *Finite Elements in Analysis and Design*, vol. 40, pp. 1599–1617, 2004.
- [6] K. Chand, L. Diachin, C. Ollivier-Gooch, E. Seol, M. Shephard, T. Tautges, and H. Trease, “Toward interoperable mesh, geometry and field components for pde simulation development,” *Engineering with Computers*, vol. 24, pp. 165–182, 2008.
- [7] M. Berger and S. Bokhari, “A partitioning strategy for nonuniform problems on multiprocessors,” *IEEE Transactions on Computing*, pp. 570–580, 1987.
- [8] J. Bentley, “Multidimensional binary search trees used for associative searching,” *Communications of the ACM*, vol. 18, pp. 509–517, 1975.
- [9] R. P. Pawlowski, J. N. Shadid, T. M. Smith, E. C. Cyr, and P. D. Weber, “Drekar::CFD - a turbulent fluid-flow and conjugate heat transfer code: Theory manual (version 1.0),” Sandia Technical Report SAND2012-2697, Sandia National Laboratories, P.O. Box 5800, Albuquerque, NM 87185, March 2012.
- [10] T. M. Evans, A. S. Stafford, R. N. Slaybaugh, and K. T. Clarno, “Denovo: a new three-dimensional parallel discrete ordinates code in SCALE,” *Nuclear Technology*, vol. 171, p. 171200, 2010.
- [11] J. Shadid, A. Salinger, R. Pawlowski, P. Lin, G. Hennigan, R. Tuminaro, and R. Lehoucq, “Large-scale stabilized FE computational analysis of nonlinear steady-state transport/reaction systems,” *Computer Methods in Applied Mechanics and Engineering*, vol. 195, pp. 1846–1871, 2006.